Zeolite Minilith: A Unique Structured Catalyst for the Methanol to Gasoline Process

Toyin Omojola[a,b,*], Nikolay Cherkasov[b], Evgeny V. Rebrov[b], Dmitry B. Lukyanov[a], Semali P. Perera[a,*]

[a] Department of Chemical Engineering, University of Bath, Claverton Down, Bath, BA2 7AY, UK
[b] School of Engineering, University of Warwick, Library Road, Coventry, CV4 7AL. UK

Corresponding authors: o.omojola@bath.ac.uk, s.perera@bath.ac.uk

Abstract

Structured microchannel H-ZSM-5 catalysts containing up to 80 wt% zeolite (balance bentonite) were fabricated by unit operations of paste preparation, extrusion, drying and firing. The structured catalysts, called miniliths due to their micrometre-range dimensions, were composed of parallel cylindrical channels with a wall thickness of 200 – 300 μm, density of 2.1 channels/mm^2 and a channel diameter of 300 μm. These miniliths were characterised by X-ray diffraction, scanning electron microscopy, energy dispersive X-ray analysis, N_2 physisorption and thermogravimetric analysis. For the first time, these miniliths were tested for the conversion of methanol to gasoline at 370 °C, 3 bar and a weight hourly space velocity (WHSV) of up to 1170 h^{-1}. A gasoline product yield of 53% was obtained at a methanol conversion of 74% over the ZSM-5 miniliths. The pressure drop at the same conversion over a packed-bed reactor of equal ZSM-5 content was 2 orders of magnitude higher than that of the minilith. Reducing the amount of ZSM-5 catalyst in the packed bed, to obtain similar inlet pressure as the ZSM-5 minilith gave the same product yield at a much higher conversion (81%) demonstrating the potential of these structured microchannel reactors.

Keywords: methanol-to-gasoline, methanol-to-olefin, ZSM-5, minilith, gasoline, methanol, structured reactor, micromonolith

ORCID information:

Toyin Omojola: 0000-0001-9376-6977

Nikolay Cherkasov: 0000-0001-5979-8713

Evgeny V. Rebrov: 0000-0001-6056-9520

1. Introduction

In heterogeneous catalysis, product selectivity is regulated by an interaction of mass and heat transport, kinetics and hydrodynamics. This interaction can be particularly pronounced in constrained environments such as zeolites. Zeolites, which generally possess a well-defined pore architecture and size (1), are synthesised in their powder form and used in their pelletised form in packed bed reactors. The major drawbacks to this approach are (i) high pressure drop, (ii) limited use of catalyst bed, (iii) flow maldistribution (e.g. channelling) and (iv) heat- and mass-transport limitations (2, 3). The high pressure drop is circumvented by using larger pellets that increase the inter-particle channel dimensions. Large pellets, however, lead to intra-pellet mass transfer limitations. Flow maldistribution is minimised by ensuring a high ratio of the reactor diameter to catalyst particle diameter (4-6). The need for small particle sizes and low pressure drop can be decoupled using a structured reactor such as a monolith (3).

The conversion of methanol to gasoline (MTG) over a packed-bed of ZSM-5 catalysts is an exothermic (1.74 MJ $kg_{methanol}^{-1}$) reaction (7, 8) with an adiabatic temperature rise of 600 °C observed in industrial packed-bed processes (8). The temperature rise in the reactors is kept within acceptable limits by separating the overall MTG process into two stages: dehydration of methanol to dimethyl ether (DME), and conversion of this mixture to hydrocarbons (9). The temperature rise in the second stage may be further reduced by applying a large recycle of gas, but this approach increases the operating costs. High exothermicity of the MTG reaction at full conversion leads to the presence of hot spots along the catalyst bed which generate uneven concentration distribution and facilitate catalyst deactivation; both resulting in an uncontrollable product selectivity. Thus, industrially, there is a demand for catalysts that: (i) show slow deactivation and (ii) allow for quick heat transfer leading to further reduction in operating costs. There has also been a long standing scholarly debate on the formation of primary products from methanol either directly (10-18) or through a hydrocarbon pool mechanism (19-27). Studying the induction period or steady state MTG conversion at low contact times can allow for mechanistic investigations of primary product formation.

A reduced probability of hot spots is obtained due to high reproducibility of size and surface characteristics of individual monolithic passages that allow for equal flow, mass and heat transport conditions under adiabatic operation (2). Short-length monoliths are used to enhance mass and heat

transfer as velocity, temperature and concentration profiles are still developing (2). It is well established that for simultaneously developing flow, the fluid velocity, velocity gradients, and temperature gradients near the wall in the entrance region will be higher than that attained with fully developed profiles. Consequently, the higher velocities convect more thermal energy in the flow direction, and heat transfer in the thermal entrance region is higher for the case of developing velocity profiles (28).

Zeolite-coated spheres (29), zeolite membranes (30), ceramic foams (31), β-SiC foams (32), wash-coated monoliths (33, 34) have been used to intensify the conversion of methanol to hydrocarbons (MTH). In all these systems, catalyst inventory remains, however, an important obstacle. This challenge can be overcome by co-extrusion of the catalyst substrate and a binder (2). Hargreaves and Munnoch (35) showed that binders can affect catalytic processes by modifying coking characteristics, entrapping poisons, transferring chemical species to or from the active phase, modifying heat transfer and porosity characteristics and improving physical durability. Whiting et al. (36) used microspectroscopy to show aluminium migration in ZSM-5-containing Al_2O_3-bound extrudates, forming additional Brønsted acid sites. Fougerit et al. (37) attributed the increase in the stability of a dealuminated mordenite catalyst for methanol to olefin conversion to the trapping of coke precursors in the binder phase. Shihabi et al. (38) showed that an α-alumina monohydrate binder inclusion on a siliceous H-ZSM-5 catalyst significantly enhanced the conversion of methanol to hydrocarbons. This enhancement was attributed to the transfer of aluminium species from the binder to the zeolite phase.

In this contribution, we fabricated, characterised and tested a co-extruded structured catalyst with micrometre-range channels for MTG conversion. The structured catalysts, extruded into a cylindrical form, contained the ZSM-5 catalyst in the bulk and on the outer surface of the channels. The structured catalysts referred to as ZSM-5 miniliths have a potential industrial significance as they not only reduce the pressure drop (thereby reducing operating costs) but also maintain high catalyst loading. These advantages have been achieved with similar gasoline yields as those obtained under reported industrial conditions. Also, the dimensions of short microchannels allow for the accessibility of very low residence times (39) which could be relevant to solving the initial C-C bond conundrum in the absence of transport restrictions.

2. Material and Methods

2.1. Catalyst preparation

A commercial NH_4-ZSM-5 zeolite catalyst with a Si/Al ratio of 25 was purchased from Zeolyst International. The catalyst powder was sieved (0.5 mm mesh) to remove larger particles and mixed with 20 – 50 wt% sodium bentonite powder received from RS minerals Ltd. The total solid weight (ZSM-5 and bentonite) was 100 g. Distilled water was added to the zeolite-bentonite mixture. The optimum water weight was found to be in the range from 0.9 (sample D) to 1.2 (sample A) times the weight of the solid mixture. The resulting paste was homogenised in a high-shear mixer (Clatronic, 1000W) for 2 min. Since the water content varied with binder content, the ZSM-5/bentonite ratio was altered to study its influence on pore volume and surface area. The compositions studied are listed in Table 1. For sample A2, 10 g of carbon (activated carbon, Nuchar) was added to the solid mixture. Sample B can also be compared to B2 to investigate the effect of water content as they both contain equal ZSM-5 and bentonite content.

The wet homogenous paste was kneaded to remove trapped air and extruded manually through a cylindrical multi-pin die with a bench mounted press. The extrudates, which possess micrometre-range channels, are called miniliths. The term, minilith, has been used before to refer to structured hydrodemetalation catalysts (40, 41). The minilith were further dried in a cold room (5 °C) and were rolled around periodically to ensure homogenous drying in accordance with the method used by Lee et al. (42). The dried minilith extrudates were heated in a kiln (Rohde) at 5 °C min^{-1} up to 450 °C and held for 0.5 h. This temperature was chosen to preserve the mechanical strength of the minilith while maintaining the distribution of acid sites between Brønsted and Lewis acid sites (43).

Table 1: Composition of the ZSM-5 miniliths

Sample code	ZSM-5 (g)	Bentonite (g)	Carbon (g)	Water (g)
A	50	50	-	121
B	60	40	-	111
C	70	30	-	91
D	80	20	-	91
A2	50	50	10	137
B2	60	40	-	82

2.2. Catalyst characterisation

The minilith samples were ground and X-ray diffraction (XRD) studies were performed with a Bruker Advance D8 diffractometer using Cu $K_{\alpha 1}$ radiation equipped with standard Bragg-Brentano geometry. Nitrogen physisorption studies were carried out on the unground samples with a Micromeritics ASAP 2020 unit. The samples were degassed by heating to 300 °C under vacuum (10^{-6} mbar) for 8 h. After degassing, nitrogen was adsorbed at -196 °C at increasing partial pressures to determine the BET surface area and the pore volume. A Rouquerol-adjusted BET surface area (44) was then calculated. The morphology and elemental analysis were obtained using energy dispersive X-ray analysis of the zeolite minilith was studied using a JEOL (JSM-6480LV) scanning electron microscope equipped with an Oxford INCA X–act 10 mm^2 SDD X-ray detector.

Thermogravimetric analysis (TGA) of the ground miniliths as well as the original ZSM-5 catalyst and bentonite powder was carried out in a Setsys Evolution TGA 16/18 instrument (SETARAM). Before each experiment, 12 mg of sample was placed into an alumina crucible held in a TGA chamber that was purged with air at 20 °C at 200 mL min^{-1} for 8 min. All gas flow rates refer to normal temperature and pressure. The experiments were performed under air flowing at 20 mL min^{-1} at a heating rate of 5 °C min^{-1} to the temperature of 600 °C.

2.3. ZSM-5 minilith catalytic tests

The ZSM-5 minilith (~ 3.9 mm O.D, 14 mm length) was placed between two quartz wool plugs and inserted in a cylindrical quartz tube (4 mm I.D, 6 mm O.D). The quartz tube was housed in a heater (see Fig. S1 in supplementary information). To obtain the H-form, the NH_4-ZSM-5 minilith was additionally calcined under oxygen flow at 450 °C for 30 min at a heating rate 5 °C min^{-1}. This additional calcination was conducted to ensure the same integrity of miniliths used in catalytic tests. Thereafter, the ZSM-5 minilith was purged with nitrogen at a flowrate of 10 mL min^{-1} while the reactor temperature was brought down to 370 °C. During the MTG reaction, nitrogen was passed at various flowrates through a vessel containing methanol which was immersed in a saturator at 4.2 °C. A back-pressure controller was used to maintain an inlet pressure of 3 bar. The reaction products were sampled through

an online gas chromatography (Shimadzu GC 2010) equipped with a flame ionisation detector and an Equity-1 fused silica capillary column (90m × 0.53mm × 3.0µm).

The methanol conversion and yield were calculated on a carbon basis. The conversion was defined as the fraction of oxygenates consumed during the reaction (equation 1), where $C_{MeOH,in}$ is the inlet methanol mole concentration, $C_{oxy,out}$ is the sum of the outlet mole concentrations of methanol and twice the outlet mole concentrations of DME. C_i is the mole concentrations of species (ethene, propene etc)

$$X = \frac{C_{MeOH,in} - C_{oxy,out}}{C_{MeOH,in}} \times 100\%, \quad (1)$$

Dry yield towards hydrocarbons was calculated based on carbon number. For instance, for ethene and propene, it is given as:

$$Y_{ethene} = \frac{2 \cdot C_{C2H4}}{C_{MeOH,in}} \times 100\%, \quad (2)$$

$$Y_{propene} = \frac{3 \cdot C_{C3H6}}{C_{MeOH,in}} \times 100\%, \quad (3)$$

The product distribution (mass fraction, w_i) of species was evaluated as:

$$w_i = \frac{m_i}{\sum m_c + m_{H_2O} + m_{N_2}} \quad (4)$$

Where m_i is the mass of specie, i, m_c is the total mass of hydrocarbons (aliphatics and aromatics), m_{H2O} is the water mass and m_{N2} is the mass of carrier gas, N_2. The calculation of mass and moles of species are given in a sample calculation in Table S1 in supplementary information.

A test experiment on the effect of the binder was conducted at 370 °C and the lowest flow rate of 54 mL min^{-1}. Additionally, stability measurements were conducted over a chosen minilith (Sample C) and compared to a zeolite/bentonite mixture of equal ZSM-5 weight at 3 bar and a flowrate of 54 mL min^{-1}.

3. Results and discussion

3.1. Catalyst characterisation

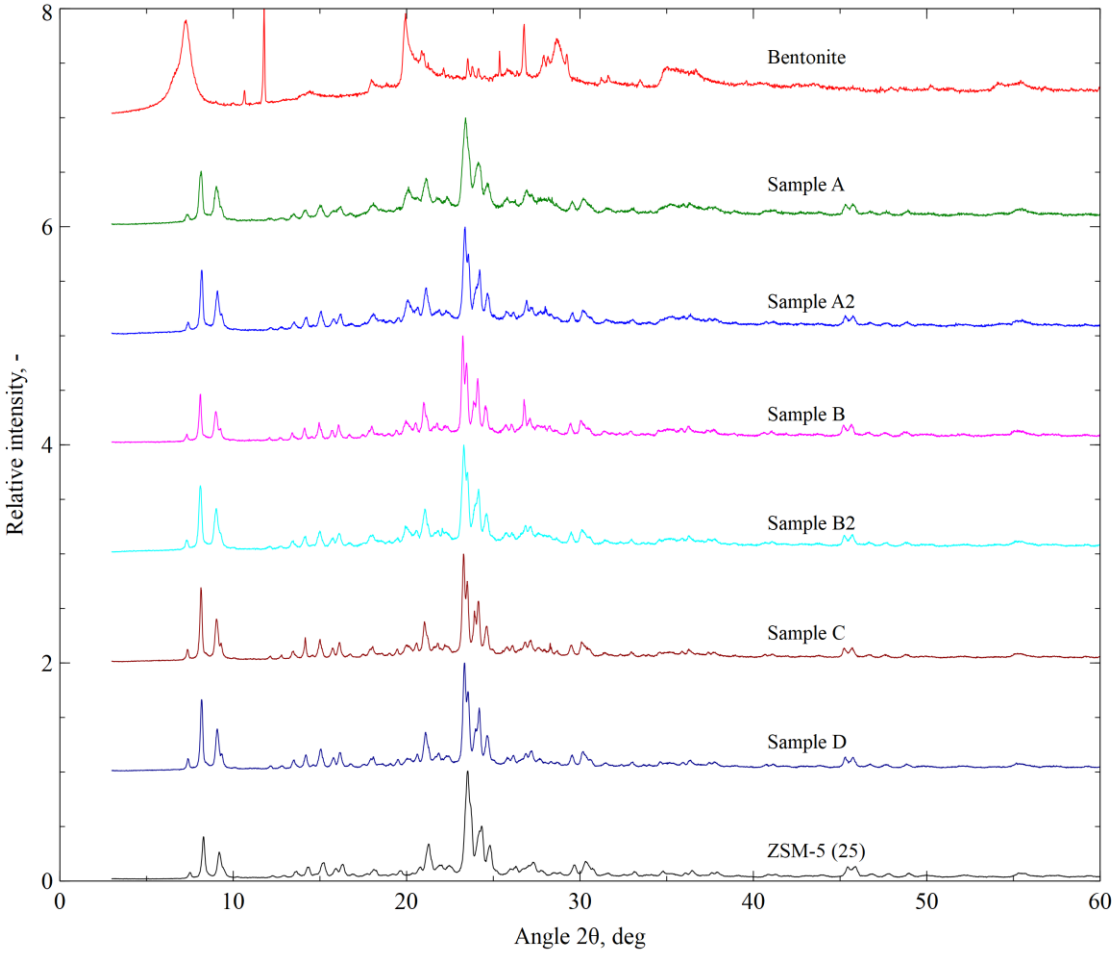

Fig. 1: Powder X-ray diffraction patterns of bentonite, ZSM-5 miniliths and ZSM-5 catalyst.

The XRD patterns of the miniliths composed of ZSM-5 and bentonite are presented in Fig. 1. All samples exhibit the MFI structure with major peaks located at *2θ* about 7.9° and 8.9° and the characteristic triplet at 23.5° (45, 46). ZSM-5 peaks did not shift on adding bentonite. Carbon as a pore template does not affect lattice crystallinity. This is because during firing the carbon is burnt-off to create mesoporosity. Carbon affects the porosity (as shown in Table 2) but not the crystallinity.

Table 2: Porosity data of the ZSM-5 miniliths

Sample code	ZSM-5 (g)	Bentonite (g)	Carbon (g)	Water (g)	BET$^{\Omega}$ surface area, $m^2\ g^{-1}$	HK* micropore volume, $cm^3\ g^{-1}$	Total pore volume, $cm^3\ g^{-1}$	Si/Al ratio
A	50	50	-	121	293	0.114	0.175	7.6
B	60	40	-	111	273	0.109	0.183	9.4
C	70	30	-	91	323	0.129	0.235	11.7
D	80	20	-	91	353	0.142	0.238	14.6
A2	50	50	10	137	224	0.075	0.132	7.7
B2	60	40	-	82	279	0.111	0.193	10.2
ZSM-5	100	-	-	-	419	0.143	0.222	25$^{\Delta}$
Bentonite	-	100	-	-	48	0.013	0.048	1.5$^{\Delta}$

$^{\Omega}$Rouquerol-adjusted BET values. *HK:Horvath-Kawazoe. $^{\Delta}$Commercial values.

ZSM-5 and bentonite both have micropores (below 2 nm in diameter) and mesopores (2-50 nm in diameter). An increasing amount of bentonite added to a minilith generally reduces the BET surface area and micropore volume (Table 2). The addition of carbon to the ZSM-5/bentonite mixture to induce mesoporosity leads to a decrease in BET surface area and a decrease in micropore volume (comparing sample A to A2). This is probably due to the formation of larger pores in the minilith (see Fig. S2 in supplementary information). These macropores are formed during the burning-off of carbon during firing. Carbon agglomeration occurs during paste preparation leading to large pores on burning-off. The water content varied systematically with solid weight (ZSM-5 and bentonite). When solid weight content was kept constant (sample B vs B2), addition of more H_2O to the paste made little impact on the minilith microporosity but a higher impact on total pore volume. The Si/Al ratios of the final miniliths increases as the ZSM-5 content increases.

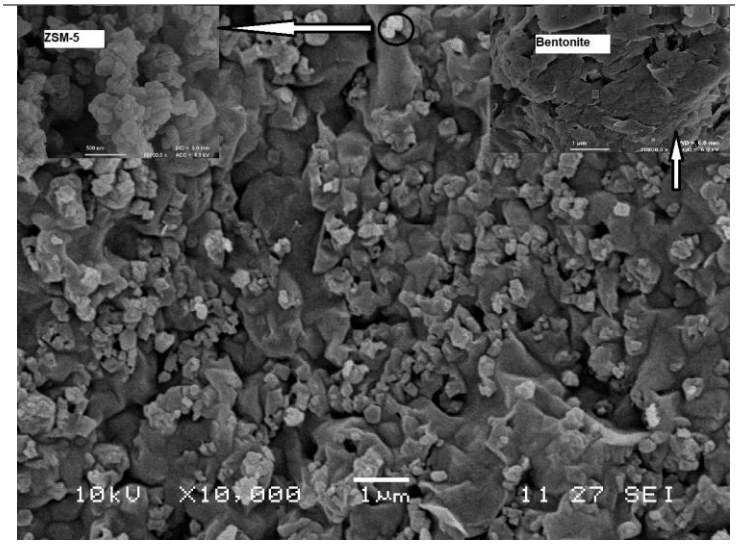

(a) A vertical cross-section of 50 wt% ZSM-5 (sample A) minilith showing an insert of the bentonite phase and ZSM-5 phase

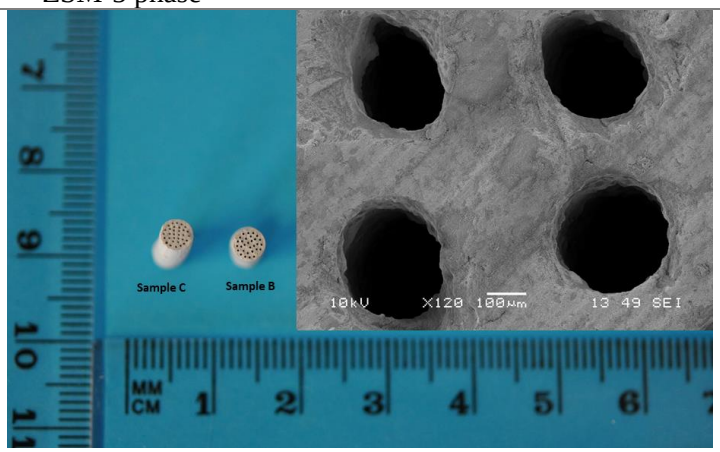

(b) Image of three minilith structures (L-R): 70 wt% (sample C) and 60 wt% ZSM-5 (sample B) with an inset of a horizontal cross-section of 70 wt% minilith (sample C)

Fig. 2: Scanning electron micrographs and images of the ZSM-5 miniliths

The scanning electron micrographs (Fig. 2) show that the ZSM-5 particles are homogeneously dispersed on the bentonite structure. The ZSM-5 particles appear as tiny islands on the flat bentonite surface. Addition of carbon leads to large cavities in the ZSM-5 minilith (comparing sample A to A2). Before firing, the ZSM-5 minilith maintains a diameter of 4.4 mm. After firing, the channels shrink in accordance to the amount of bentonite present in the structure. For instance, visual inspection of the minilith diameters before and after firing show that a 13% shrinkage occurs with 70 wt% ZSM-5 (sample C).

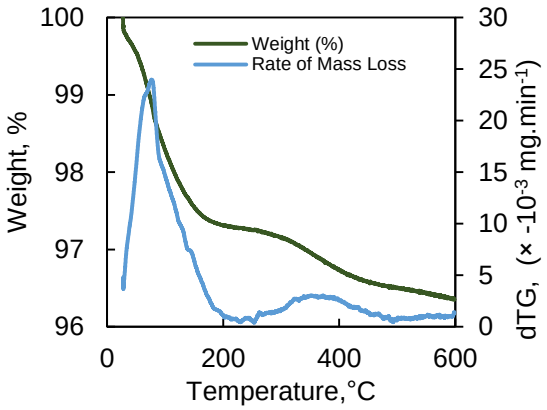

a. TGA of ZSM-5 used for ZSM-5 minilith preparation

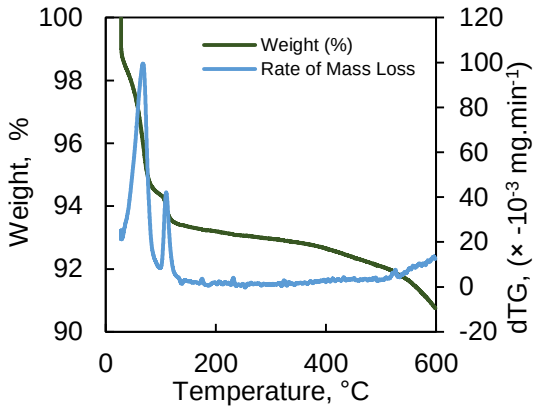

b. TGA of bentonite used for ZSM-5 minilith preparation

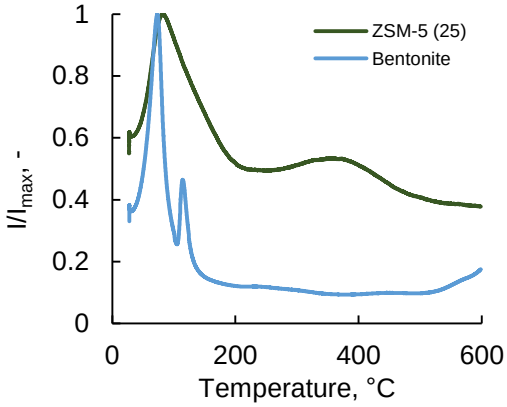

c. The release of H_2O at m/z=18 during TGA analysis

Fig. 3: TGA of weight loss (a, b) and (c) rate of H_2O release over ZSM-5 and bentonite.

Fig. 3a shows TGA curves for ZSM-5 where weight losses occur in two temperature ranges investigated: below 200°C and between 200 and 450 °C after which no weight changes are observed indicating that a stable zeolite is obtained. For bentonite, three weight loss temperature regions were obtained: below 100 °C, between 100 and 150 °C and at temperatures greater than 515 °C (Fig. 3b). The H_2O profiles (Fig. 3c) are similar in shape to the rate of mass loss profiles (Figs. 3a and b) suggesting that H_2O accounts for most of the sample loss. The bentonite weight loss below 150°C corresponds to the removal of adsorbed and interlayer water while the loss at temperatures above 515°C relates to the removal of water from bentonite (47). Therefore, prior to catalytic testing, the catalysts were fired at 450 °C to keep the chemical nature of the bentonite. This temperature is also enough to decompose the ammonium form of zeolite.

3.2. Catalytic tests

The characterisation studies show that it is possible to obtain miniliths with controlled ZSM-5 loading and porosity. All the miniliths maintained the extruded morphology with mechanical stability required for characterisation. Therefore, the MTG conversion could be performed with any minilith considering the catalyst loading, reactor dimensions and heat transfer. For a small-scale laboratory test, where heat transfer effects are less pronounced (*vide supra*), we selected minilith C to maintain a high ZSM-5 loading while keeping a reduced effect of the Si/Al ratio of bentonite on methanol to gasoline production. Although sample D had the highest ZSM-5 loading, sample C was more mechanically stable due to its higher bentonite content. A test experiment was carried out on the effect of bentonite on MTG conversion. A methanol conversion of only 0.9 % was obtained at 54 mL min^{-1}. This conversion is *ca.* 100 times lower compared to the conversion obtained under the same conditions over the minilith of similar bentonite content. Therefore, the effect of bentonite on MTG reaction over the minilith studied was negligible.

Fig. 4 shows the results of the catalytic test conducted over a minilith with 70 wt% ZSM-5 catalyst. As contact time increases, mass fractions of methanol decrease while DME rises until 5.3 g_{cat} g_{feed}^{-1} s showing the activation of the methanol dehydration reaction. Consequently, the mass fraction of H_2O rises. As contact time increases further, DME mass fraction decreases as it is involved in the chemistries of MTH chemistries such as olefin and aromatic methylation reactions (48).

The conversion of methanol to hydrocarbons is well established to be an autocatalytic reaction over ZSM-5 catalyst (49-51). The data on MTG reaction over the minilith show autocatalytic behaviour with a projected non-linear increase from zero contact times (Fig. 4). At low temperatures and high Si/Al ratios where kinetics control the rate of methanol conversion, Ono and co-workers (51) observed that the accumulation of reactive intermediates is responsible for the conversion jump as contact time is increased. This is due to the involvement of reactive species in methylation reactions. Also, rapid heat generation could be responsible for the conversion jump due to the increasing exothermicity of MTH conversion as contact time increases. The data (Fig. 4) shows that autocatalysis occurs over ZSM-5 miniliths but with the conversion jump occurring at much lower contact times. The binder acts as a heat sink by moderating temperature rise, heat generation and reaction conversion (35). Consequently, with a constant temperature across the short-length ZSM-5 minilith during MTG conversion (see

section 1), the data suggests that a low concentration of autocatalysing species is necessary to initiate the conversion jump.

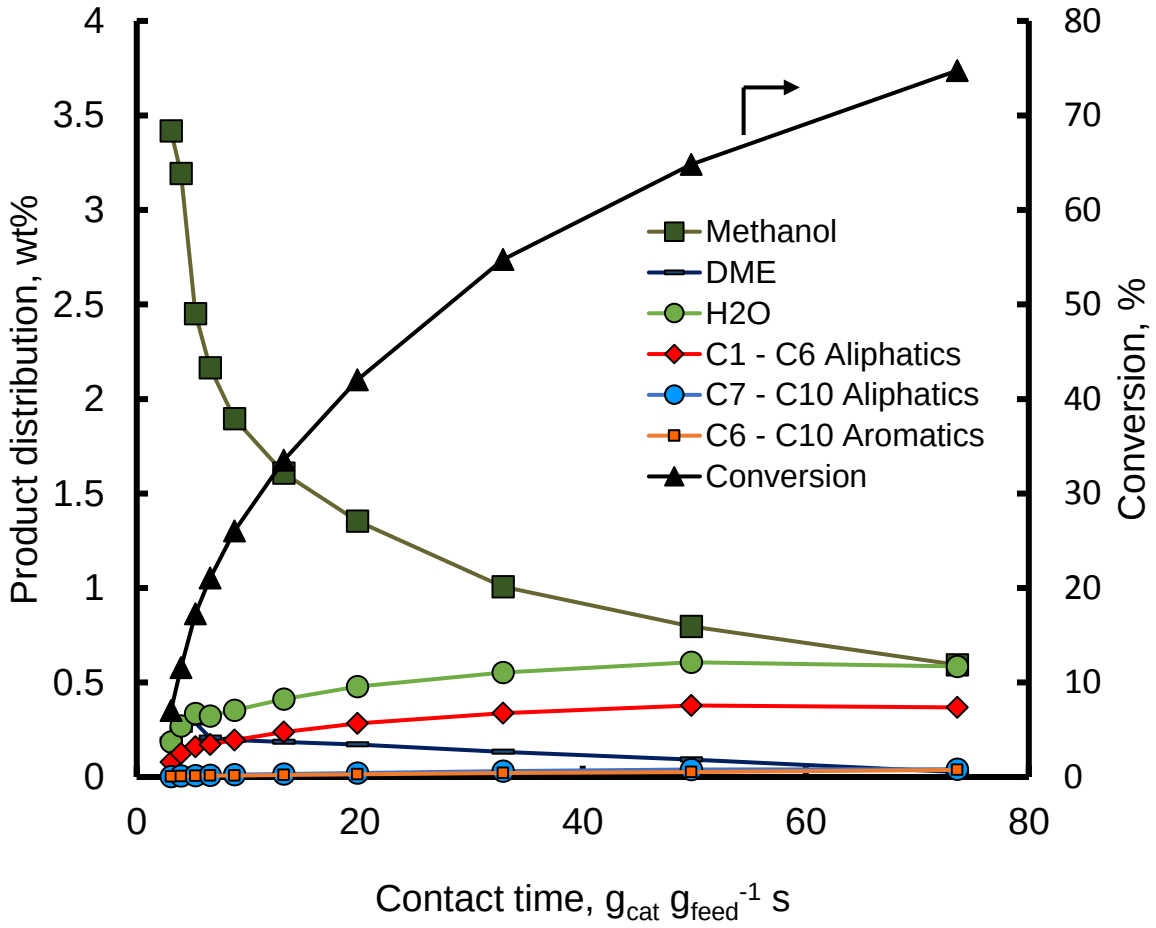

Fig. 4: Product distribution and conversion with contact time over ZSM-5 minilith (sample C) at 370 °C and an inlet pressure of 3 bar. Methanol, DME, C1-C6 aliphatics, C7 –C10 aliphatics and C6 – C10 aromatics were obtained experimentally. H_2O was calculated.

Fig. 4 also shows a rise in aliphatics and aromatics as contact time is increased. Recently, it was shown that DME is the main methylating agent present at conditions required for MTG conversion (52, 53). At high contact times, any DME produced from the equilibration reaction is fully consumed for aliphatic and aromatic production. During this period, the mass fraction of methanol falls until it reaches a plateau. Thus, DME acts as an intermediate between methanol and products (aliphatics and aromatics). DME concentration goes through a maximum because at first it is produced via the equilibration reaction (which is predominant at early contact times) and then converted into products (aliphatics and aromatics) during which it is also used as a methylating agent. The equilibration reaction leads to a

continuous depletion of methanol while DME is increasingly consumed as contact time increases. This implies that the equilibrium product concentrations can be attained at high contact times.

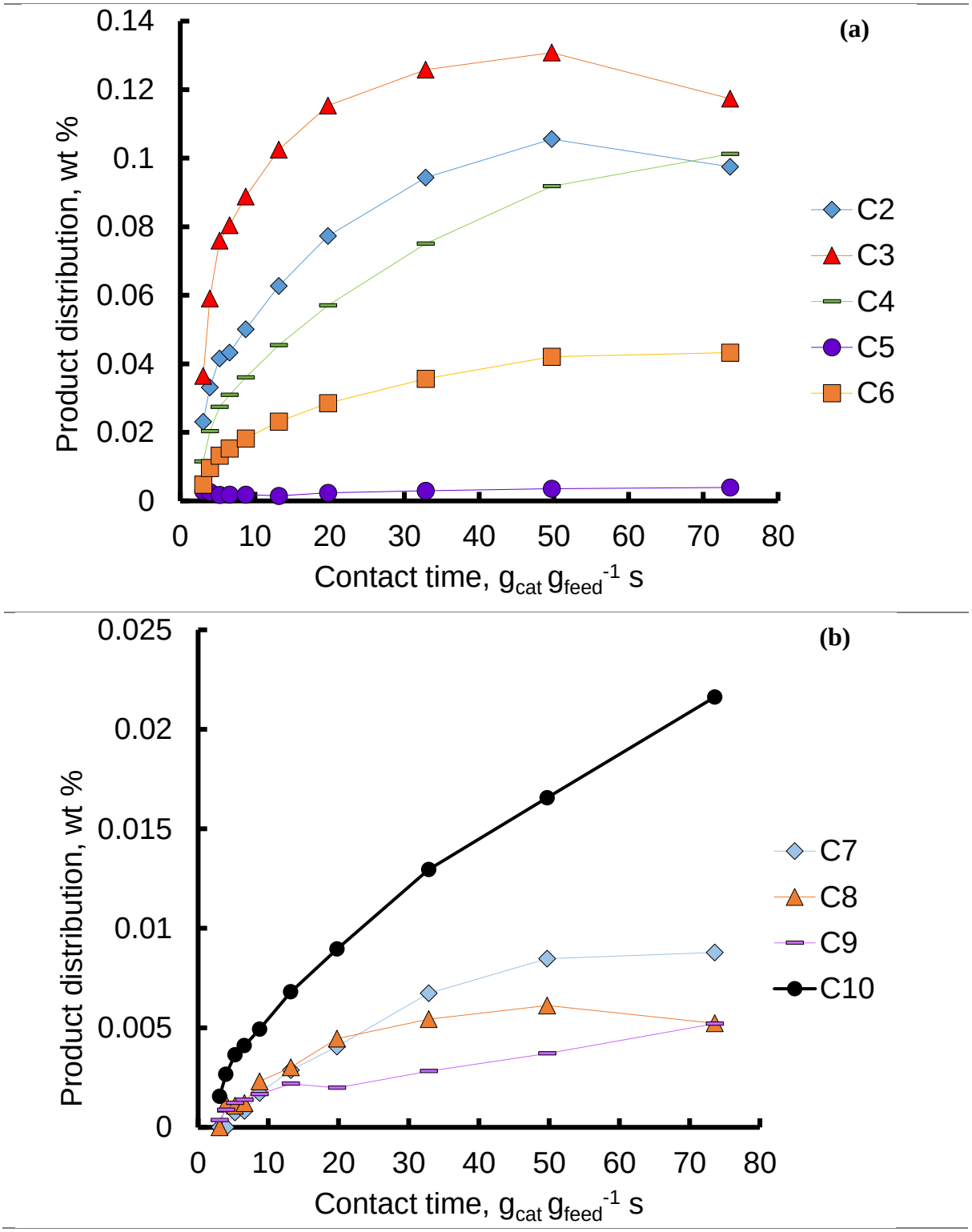

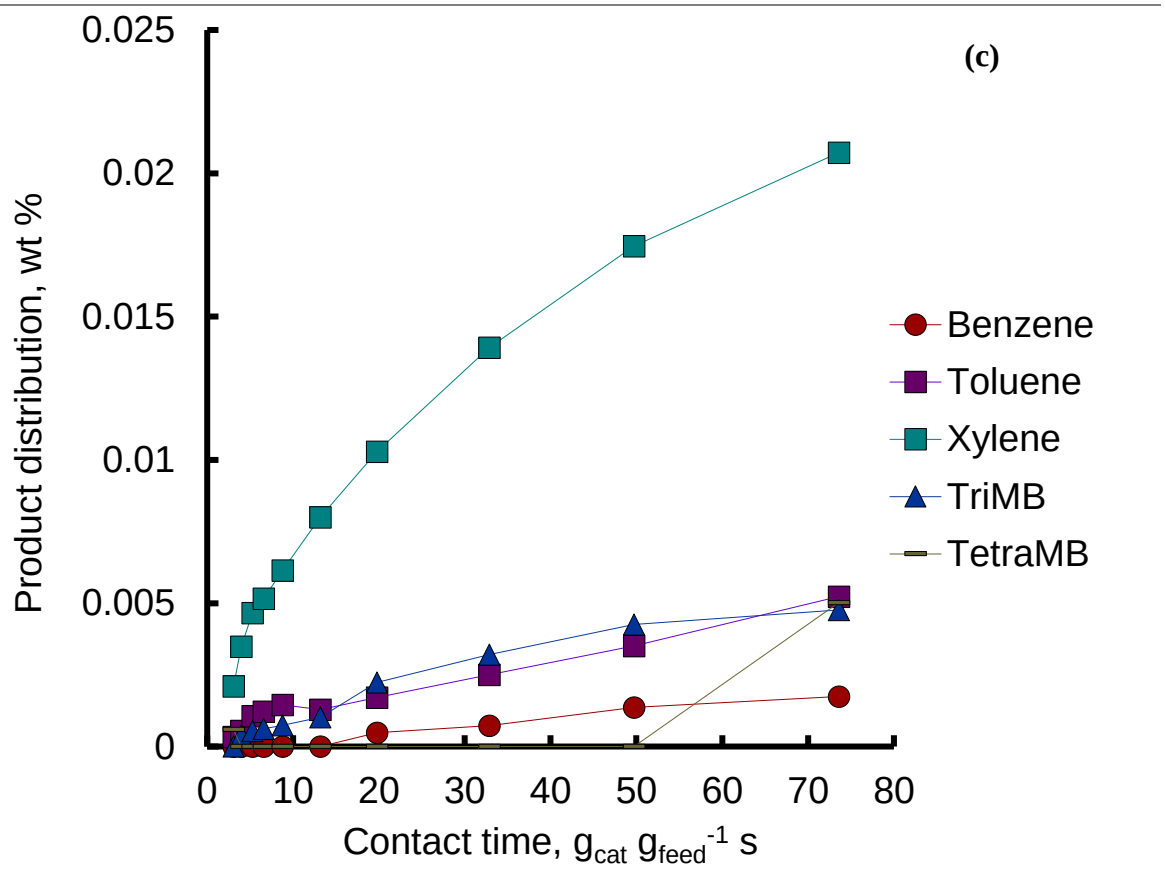

Fig. 5: (a) Aliphatic C2-C6, (b) aliphatic C7-C10 and (c) aromatics product distribution with contact time over ZSM-5 minilith (sample C) at 370 °C and 3 bar.

231 Fig. 5 shows how product distribution varies as contact time is increased. At the lowest contact
232 time of 3.1g_{cat} g_{feed}^{-1} s, a diverse range of primary products are observed. As short miniliths would allow
233 for both low residence times and efficient heat and mass transfer due to developing profiles in the
234 channels, the varied product distribution at low contact times is likely due to an established hydrocarbon
235 pool within the ZSM-5/bentonite pore wall (19-21). With comparisons made between the time taken
236 for species to travel through the axial length of the minilith and the time required to diffuse radially to
237 the surface of the channel, bulk of the minilith or to active sites on the zeolite crystal surface, the product
238 distribution obtained at low contact times is subjected to intracrystalline diffusion limitations. The
239 presence of active species in the hydrocarbon pool at low contact times corresponds with conversion
240 profiles depicted in Fig. 4. As contact time increases, a range of aliphatics and aromatics are formed.
241 The underlying mechanism involves a complex interaction of oligomerisation, methylation, hydrogen
242 transfer and cracking chemistries which are responsible for the olefin product distribution (48, 54).
243 Aliphatics are formed at lower contact times during MTG conversion. As the contact time increases,

aromatics are formed via hydrogen transfer and cyclisation reaction between methanol and olefins (55) or between olefins (56). The presence of aromatics (hydrogen-poor) at short contact times imply that paraffins (hydrogen-rich) are additionally formed from olefins. Initially, the proportion of olefins grow and at higher contact times, C2 and C3 hit a maximum and fall while C4 and C6 continue to grow. This could be due to (i) formation of C2 and C3 from primary oxygenates as well as their methylation and oligomerisation and (ii) C6 aromatisation. C6 aromatisation results in the formation of alkanes and aromatics. As contact time increases, aromatic methylation and dealkylation play an increasing role in MTG conversion and also regulate product distribution (48).

At highest conversions, the product distribution consists predominantly of C4 and C10 aliphatics and xylene aromatics which are in the gasoline boiling range and are expected from bare ZSM-5 catalysts (7). The product yield of C4 to C10 range of aliphatics and aromatics account for 53% of the dry product distribution at the highest conversions (73.6%) in this study. This is comparable with the gasoline yields obtained from bench-scale studies (57).

Pressure drop through the packed bed of ZSM-5 catalysts and one ZSM-5 minilith channel were calculated using the Ergun (58) and Hagen-Poiseuille (59, 60) equations. At a weight hourly space velocity of 273 h^{-1}, the pressure drop through the packed bed of zeolite catalysts was 2 orders of magnitude higher than that through the zeolite minilith of equal ZSM-5 weight. This difference is representative of all flowrates. It was challenging to compare the performance of zeolite powders directly to miniliths of similar ZSM-5 active weight due to differences in pressure drop through the reactor. Nonetheless, Fig. S3 (see supplementary information) shows a comparison of conversions obtained over ZSM-5 powder and miniliths (sample C). Similar conversions are obtained over both systems (ZSM-5 powder and minilith) at 13.2 and 19.8 $g_{cat}\, g_{feed}^{-1}$ s albeit at a pressure drop of 2 orders of magnitude lower with ZSM-5 minilith. The difference in pressure drop is in accordance with literature (61-63). While the conversion data obtained over the miniliths were investigated under similar inlet pressures (3 bar), there was a variation in inlet pressure for the packed bed leading to an irregular conversion with contact time profile. A long duration stability experiment comparing zeolite minilith to powder of equal ZSM-5 weight at 49 h^{-1} shows higher stability for the powder than the minilith (Fig. S4). Consequently, higher conversions are obtained over the minilith up until 40 h beyond which the

powders outperform the minilith in stability. As discussed above, packed beds show significant practical limitations associated with a higher pressure drop at high catalyst loading. Moreover, a higher minilith stability can be obtained by using a larger amount of pore-formers or different binders to prevent the slip wall condition obtained during extrusion.

Simulations conducted by Guo et al. (64), on comparing the conversion of methanol to propene over a packed bed of ZSM-5 particles to an extruded monolith, show a higher reactor efficiency and propene selectivity for monoliths. In this study, reducing the catalyst inventory to allow for equal inlet pressures of 3 bar gives the same gasoline product yield (53%) at a higher conversion of 80% over a packed bed of catalyst. This further highlights the high performing potential of ZSM-5 miniliths. Future work would elaborate on characterizing transport effects in miniliths during hydrocarbon transformations, getting an understanding on primary products formed at much lower contact times and minilith design optimisation to facilitate longer lifetime.

4. Conclusions

A novel form of a structured catalyst was prepared using a bentonite binder and ZSM-5 catalyst powder and then evaluated for the conversion of methanol to gasoline. The results of this study demonstrate that the conversion of methanol to gasoline can be performed with the ZSM-5 minilith reactor. The miniliths retain the crystal structure of the ZSM-5 catalyst and increase in Si/Al ratio, surface area and pore volume with an increase in zeolite content. The product distribution obtained over the ZSM-5 minilith reactor is in the gasoline range and similar to that obtained over ZSM-5 powder catalysts. The minilith achieves similar conversions at a pressure drop two orders of magnitude lower than with zeolite powder of equal ZSM-5 weight.

5. Author information

Corresponding Authors: o.omojola@bath.ac.uk, s.perera@bath.ac.uk

6. Acknowledgements

T. Omojola is grateful to the Petroleum Technology Development Fund of Nigeria for funding (PTDF/ED/PHD/OO/766/15) and to Dr Javier Fernandez-Garcia (University of Leeds, UK) for fruitful discussions. All data created during this research are openly available from the University of Bath Research Data Archive at https://doi.org/10.15125/BATH-00524.

7. Notes

The authors declare no competing financial interest.

8. References

1. Wright PA. Microporous framework solids. Cambridge: RSC; 2008.
2. Cybulski A, Moulin J. Monoliths in Heterogeneous Catalysis. Catalysis Reviews. 1994;36(2):179-270.
3. Pangarkar K, Schildhauer TJ, Van Ommen JR, Nijenhuis J, Kapteijn F, Moulijn JA. Structured packings for multiphase catalytic reactors. Ind Eng Chem Res. 2008;47(10):3720-51.
4. Rase HF. Chemical Reactor Design for Process Plant, Vol. 1: Principles and Techniques. New York: Wiley; 1977.
5. Richardson JT. Principles of Catalyst Development. New York: Plenum Press; 1989.
6. Satterfield CN. Heterogeneous Catalysis in Practice. New York: McGraw-Hill; 1980.
7. Chang CD, Silvestri AJ. The conversion of methanol and other O-compounds to hydrocarbons over zeolite catalysts. J Catal. 1977;47(2):249-59.
8. Keil FJ. Methanol-to-hydrocarbons: process technology. Microporous Mesoporous Mater. 1999;29(1):49-66.
9. Blauwhoff PMM, Gosselink JW, Kieffer EP, Sie ST, Stork WHJ. Zeolites as Catalysts in Industrial Processes. In: Weitkamp J, Puppe L, editors. Catalysis and Zeolites: Fundamentals and Applications: Springer-Verlag; 1999. 437-538.
10. Stöcker M. Methanol-to-hydrocarbons: Catalytic materials and their behavior. Microporous Mesoporous Mater. 1999;29(1-2):3-48.
11. Hunter R, Hutchings GJ. Hydrocarbon formation from methylating agents over the zeolite catalyst H-ZSM-5 and its conjugate base: Evidence against the trimethyloxonium ion-ylide mechanism. J Chem Soc, Chem Commun. 1985(22):1643-5.
12. Hutchings GJ, Gottschalk F, Hall MVM, Hunter R. Hydrocarbon formation from methylating agents over the zeolite catalyst ZSM-5. Comments on the mechanism of carbon-carbon bond and methane formation. Journal of the Chemical Society, Faraday Transactios 1: Physical Chemistry in Condensed Phases. 1987;83(3):571-83.
13. Hunter R, Hutchings GJ. Hydrocarbon formation from methanol using WO3/Al 2O3 and zeolite H-ZSM-5 catalysts: Further evidence on the reaction mechanism. J Chem Soc, Chem Commun. 1987(5):377-9.
14. Hunter R, Hutchings GJ, Pickl W. Mechanistic studies on initial C-C bond formation in the zeolite ZSM-5 catalysed methanol conversion reaction: Evidence against a radical pathway. J Chem Soc, Chem Commun. 1987(11):843-4.
15. Wang W, Seiler M, Hunger M. Role of surface methoxy species in the conversion of methanol to dimethyl ether on acidic zeolites investigated by in situ stopped-flow MAS NMR spectroscopy. J Phys Chem B. 2001;105(50):12553-8.
16. Wang W, Buchholz A, Seiler M, Hunger M. Evidence for an Initiation of the Methanol-to-Olefin Process by Reactive Surface Methoxy Groups on Acidic Zeolite Catalysts. J Am Chem Soc. 2003;125(49):15260-7.
17. Yamazaki H, Shima H, Imai H, Yokoi T, Tatsumi T, Kondo JN. Direct production of propene from methoxy species and dimethyl ether over H-ZSM-5. Journal of Physical Chemistry C. 2012;116(45):24091-7.
18. Li J, Wei Z, Chen Y, Jing B, He Y, Dong M, Jiao H, Li X, Qin Z, Wang J, Fan W. A route to form initial hydrocarbon pool species in methanol conversion to olefins over zeolites. J Catal. 2014;317(0):277-83.
19. Bjørgen M, Svelle S, Joensen F, Nerlov J, Kolboe S, Bonino F, Palumbo L, Bordiga S, Olsbye U. Conversion of methanol to hydrocarbons over zeolite H-ZSM-5: On the origin of the olefinic species. J Catal. 2007;249(2):195-207.
20. Svelle S, Joensen F, Nerlov J, Olsbye U, Lillerud KP, Kolboe S, Bjørgen M. Conversion of methanol into hydrocarbons over zeolite H-ZSM-5: Ethene formation is mechanistically separated from the formation of higher alkenes. J Am Chem Soc. 2006;128(46):14770-1.

21. Bjørgen M, Joensen F, Lillerud KP, Olsbye U, Svelle S. The mechanisms of ethene and propene formation from methanol over high silica H-ZSM-5 and H-beta. Catal Today. 2009;142(1-2):90-7.
22. Dahl IM, Kolboe S. On the Reaction Mechanism for Hydrocarbon Formation from Methanol over SAPO-34. I. Isotopic Labeling Studies of the Co-Reaction of Ethene and Methanol. J Catal. 1994;149(2):458-64.
23. Dahl IM, Kolboe S. On the reaction mechanism for hydrocarbon formation from methanol over SAPO-34: 2. Isotopic labeling studies of the Co-reaction of propene and methanol. J Catal. 1996;161(1):304-9.
24. Wang C, Xu J, Qi G, Gong Y, Wang W, Gao P, Wang Q, Feng N, Liu X, Deng F. Methylbenzene hydrocarbon pool in methanol-to-olefins conversion over zeolite H-ZSM-5. J Catal. 2015;332:127-37.
25. Svelle S, Olsbye U, Joensen F, Bjørgen M. Conversion of methanol to alkenes over medium- and large-pore acidic zeolites: Steric manipulation of the reaction intermediates governs the ethene/propene product selectivity. Journal of Physical Chemistry C. 2007;111(49):17981-4.
26. Goguen PW, Xu T, Barich DH, Skloss TW, Song W, Wang Z, Nicholas JB, Haw JF. Pulse-quench catalytic reactor studies reveal a carbon-pool mechanism in methanol-to-gasoline chemistry on zeolite HZSM-5. J Am Chem Soc. 1998;120(11):2650-1.
27. Haw JF, Nicholas JB, Song W, Deng F, Wang Z, Xu T, Heneghan CS. Roles for cyclopentenyl cations in the synthesis of hydrocarbons from methanol on zeolite catalyst HZSM-5. J Am Chem Soc. 2000;122(19):4763-75.
28. Shah RK, London AL. Laminar Flow Forced Convection in Ducts. Irvine TF, Hartnett JP, editors: Academic Press, Inc; 1978.
29. Schulz H, Lau K, Claeys M. Kinetic regimes of zeolite deactivation and reanimation. Applied Catalysis A, General. 1995;132(1):29-40.
30. Masuda T, Asanuma T, Shouji M, Mukai SR, Kawase M, Hashimoto K. Methanol to olefins using ZSM-5 zeolite catalyst membrane reactor. Chem Eng Sci. 2003;58(3-6):649-56.
31. Patcas FC. The methanol-to-olefins conversion over zeolite-coated ceramic foams. J Catal. 2005;231:194-200.
32. Ivanova S, Louis B, Madani B, Tessonnier JP, Ledoux MJ, Pham-Huu C. ZSM-5 Coatings on β-SiC Monoliths: Possible New Structured Catalyst for the Methanol-to-Olefins Process. The Journal of Physical Chemistry C. 2007;111(11):4368-74.
33. Anita JE, Govind R. Conversion of Methanol to Gasoline-Range Hydrocarbons in a ZSM-5 Coated Monolithic Reactor. Industrial Engineering and Chemistry Research. 1995;34:140-7.
34. Patil MD, Lachman IM. Methanol Conversion on Ceramic Honeycombs Coated with Silicalite. In: Flank WH, editor. Perspectives in Molecular Sieve Science. Washington D.C: American Chemical Society; 1988. 492-9.
35. Hargreaves JSJ, Munnoch AL. A survey of the influence of binders in zeolite catalysis. Catalysis Science and Technology. 2013;3(5):1165-71.
36. Whiting GT, Meirer F, Mertens MM, Bons AJ, Weiss BM, Stevens PA, De Smit E, Weckhuysen BM. Binder effects in SiO_2- and Al_2O_3-bound zeolite ZSM-5-based extrudates as studied by microspectroscopy. ChemCatChem. 2015;7(8):1312-21.
37. Fougerit JM, Gnep NS, Guisnet M, Amigues P, Duplan JL, Hugues F. Effect of the binder on the properties of a mordenite catalyst for the selective conversion of methanol into light olefins. Stud Surf Sci Catal. 1994;84:1723-30.
38. Shihabi DS, Garwood WE, Chu P, Miale JN, Lago RM, Chu CTW, Chang CD. Aluminum insertion into high-silica zeolite frameworks. II. Binder activation of high-silica ZSM-5. J Catal. 1985;93(2):471-4.
39. Divins NJ, López E, Rodríguez Á, Vega D, Llorca J. Bio-ethanol steam reforming and autothermal reforming in 3-μm channels coated with RhPd/CeO2 for hydrogen generation. Chemical Engineering and Processing: Process Intensification. 2013;64:31-7.
40. Pereira CJ, Cheng WC, Beeckman JW, Suarez W. Performance of the minilith-a shaped hydrodemetallation catalyst. Applied Catalysis. 1988;42(1):47-60.
41. Pereira CJ, Beeckman JW. Modeling of hydrodemetalation catalysts. Industrial & Engineering Chemistry Research. 1989;28(4):422-7.

42. Lee LY, Perera SP, Crittenden BD, Kolaczkowski ST. Manufacture and characterisation of silicalite monoliths. Adsorpt Sci Technol. 2000;18(2):147-70.
43. Spivey JJ. Review: Dehydration catalysts for the methanol/dimethyl ether reaction. Chem Eng Commun. 1991;110(1):123-42.
44. Rouquerol J, Llewellyn P, Rouquerol F. Is the BET equation application to microporous adsorbents? In: Llewellyn P, Rodriquez-Reinoso F, Rouquerol J, Seaton N, editors. Stud Surf Sci Catal. 160: Elsevier; 2007. 49-56.
45. van Koningsveld HV, van Bekkm H, Jansen JC. On the Location and Disorder of the Tetrapropylammonium (TPA) Ion in Zeolite ZSM-5 with Improved Framework Accuracy. Acta Crystallography. 1987;B43(Part 2):127-32.
46. Olson DH, Kokotailo GT, Lawton SL, Meier WM. Crystal structure and structure-related properties of ZSM-5. J Phys Chem. 1981;85(15):2238-43.
47. Ayari F, Srasra E, Trabelsi-Ayadi M. Characterization of bentonitic clays and their use as adsorbent. Desalination. 2005;185(1):391-7.
48. Ilias S, Bhan A. Mechanism of the catalytic conversion of methanol to hydrocarbons. ACS Catalysis. 2013;3:18-31.
49. Chen NY, Reagan WJ. Evidence of autocatalysis in methanol to hydrocarbon reactions over zeolite catalysts. J Catal. 1979;59(1):123-9.
50. Ono Y, Mori T. Mechanism of methanol conversion into hydrocarbons over ZSM-5 zeolite. Journal of the Chemical Society, Faraday Transactions 1: Physical Chemistry in Condensed Phases. 1981;77(9):2209-21.
51. Ono Y, Imai E, Mori T. The Autocatalytic Nature of Methanol Conversion over ZSM-5 Zeolites. Z Phys Chem1979. p. 99.
52. Omojola T, Cherkasov N, McNab AI, Lukyanov DB, Anderson JA, Rebrov EV, van Veen AC. Mechanistic Insights into the Desorption of Methanol and Dimethyl Ether Over ZSM-5 Catalysts. Catal Lett. 2018;148(1):474-88.
53. Svelle S, Kolboe S, Swang O, Olsbye U. Methylation of Alkenes and Methylbenzenes by Dimethyl Ether or Methanol on Acidic Zeolites. The Journal of Physical Chemistry B. 2005;109(26):12874-8.
54. Pines H. Acid-Catalyzed Reactions The Chemistry of Catalytic Hydrocarbon Conversions. United Kingdom: Academic Press; 1981.
55. Müller S, Liu Y, Kirchberger FM, Tonigold M, Sanchez-Sanchez M, Lercher JA. Hydrogen Transfer Pathways during Zeolite Catalyzed Methanol Conversion to Hydrocarbons. J Am Chem Soc. 2016;138(49):15994-6003.
56. Lukyanov DB, Gnep NS, Guisnet MR. Kinetic modeling of ethene and propene aromatization over HZSM-5 and GaHZSM-5. Ind Eng Chem Res. 1994;33(2):223-34.
57. Tabak SA, Yurchak S. Conversion of methanol over ZSM-5 to fuels and chemicals. Catal Today. 1990;6(3):307-27.
58. Ergun S. Fluid flow through packed columns. Chem Eng Prog. 1952;48(2):89-94.
59. Hagen G. Ueber die Bewegung des Wassers in engen cylindrischen Röhren. Annalen der Physik. 1839;122(3):423-42.
60. Hagenbach E. Ueber die Bestimmung der Zähigkeit einer Flüssigkeit durch den Ausfluss aus Röhren. Annalen der Physik. 1860;185(3):385-426.
61. Lachman IM, McNally RN. Monolithic Honeycomb Supports for Catalysis. Chem Eng Prog. 1985;81(1):29-31.
62. Marín P, Hevia MAG, Ordóñez S, Díez FV. Combustion of methane lean mixtures in reverse flow reactors: Comparison between packed and structured catalyst beds. Catal Today. 2005;105(3-4):701-8.
63. Lei Z, Wen C, Zhang J, Chen B. Selective catalytic reduction for NO removal: Comparison of transfer and reaction performances among monolith catalysts. Ind Eng Chem Res. 2011;50(10):5942-51.
64. Guo W, Xiao W, Luo M. Comparison among monolithic and randomly packed reactors for the methanol-to-propylene process. Chem Eng J. 2012;207-208:734-45.